Modeling of Corneal Surfaces With Radial Polynomials

D. Robert Iskander*, *Member, IEEE*, Mark R. Morelande, Michael J. Collins, and Brett Davis

***Abstract*—We consider analytical modeling of the anterior corneal surface with a set of orthogonal basis functions that are a product of radial polynomials and angular functions. Several candidate basis functions were chosen from the repertoire of functions that are orthogonal in the unit circle and invariant in form with respect to rotation about the origin. In particular, it is shown that a set of functions that is referred herein as Bhatia–Wolf polynomials, represents a better and more robust alternative for modeling corneal elevation data than traditionally used Zernike polynomials. Examples of modeling corneal elevation are given for normal corneas and for abnormal corneas with significant distortion.**

***Index Terms*—Cornea, model selection, radial polynomials, Zernike polynomials.**

I. Introduction

OVER the last decade, modeling corneal surfaces from videokeratoscopic measurements has attracted great interest among optometrists, vision scientists, and ophthalmologists. Unlike the popular dioptric power maps of corneal surfaces [1], [2], the raw height data acquired by a videokeratoscope are suitable for characterizing aberrations [3], [4] and abnormalities [5], [6] of the cornea.

Early models of the corneal anterior surfaces included simple geometric surfaces such as an ellipsoid or were generated by a polynomial curve of revolution as in the Lotmar's eye model [7]. More complex models have been used to account for corneal asymmetries. The simplest two-dimensional (2-D) model for corneal surfaces was the Taylor series expansion. This model was soon replaced by Zernike polynomials [8], which are a product of angular functions and radial polynomials.

Zernike polynomials are orthogonal for the interior of the unit circle and are invariant in form with respect to rotations of axes about the origin [9]. These properties have made Zernike polynomials very attractive in optics where they are used for fitting wavefront aberrations. Additionally, the lower terms of the Zernike polynomial expansion can be related to known types of aberrations such as defocus, astigmatism, coma, and spherical aberration [10].

Despite the good mathematical and statistical properties of Zernike polynomials, their application to the modeling of the anterior surface of the cornea does have limitations. Cases have been reported where the Zernike polynomial fit to the height data from a videokeratoscope is not adequate [11]. This is mainly because Zernike polynomials are global functions and are not suitable for characterizing local changes.

There are uncertainties as to how many Zernike terms one should fit to the data. Recently, we have developed a bootstrap based technique for fitting Zernike polynomials to corneal elevation data [12], allowing objective selection of the optimal number of Zernike terms. In a further study involving 70 subjects [13], it was concluded that the fourth-order radial fit of Zernike polynomials is adequate for judicious modeling of the majority of corneal surfaces. However, at the same time, we have observed that the residual error between the height data and the fit was slightly larger than the one observed when testing videokeratoscopes with artificial surfaces [14]. This suggests that the Zernike polynomials may not be the best option for modeling corneal surfaces.

A question arises, therefore, whether there exists a set of functions or radial polynomials that would result in a better fit to the videokeratoscopic data. We emphasize the radial polynomials because videokeratoscopes that are based on the placido disk principle acquire radial data in equally spaced meridians. This type of instruments represents a substantial majority of the current videokeratoscopes in the marketplace.

To answer the above question, we investigate alternative solutions to the problem of corneal modeling and search for a set of radial polynomials which in combination with angular functions would provide the best fit to the videokeratoscopic height data. In particular, we seek a set of radial polynomials, selected from a given repertoire, that results in a minimum mean square error (MMSE) fit to the corneal data for a given radial order.

The paper is organized as follows. In the Section II, we consider the general problem of optimal modeling of corneal surfaces by a repertoire of basis functions. In Section III, we review the possible candidate sets of basis functions that we could use in our application, and analyze their performance for simulated surfaces. Then, in Section IV, we show experimental results of fitting different radial polynomials to corneal data for subjects with normal and distorted corneas.

II. Modeling Corneal Surfaces With Polynomials

The anterior surface of the cornea can be modeled by a finite series

$$C(\rho,\theta) = \sum_{p=1}^{P} a_p \psi_p(\rho,\theta) + \varepsilon(\rho,\theta) \tag{1}$$

Manuscript received June 18, 2001; revised November 28, 2001. *Asterisk indicates corresponding author.*

*D. R. Iskander is with the School of Engineering, Griffith University, PMB 50 Gold Coast Mail Centre, Q9726, Australia. (e-mail: r.iskander@mailbox.gu.edu.au).

M. R. Morelande, M. J. Collins, and B. Davis are with the Centre for Eye Research, Queensland University of Technology, Kelvin Grove Q4059, Australia.

Publisher Item Identifier S 0018-9294(02)03003-3.

where $C(\rho, \theta)$ denotes the corneal surface, the index p is a polynomial-ordering number, $\psi_p(\rho, \theta)$, $p = 1, \ldots, P$, is the pth polynomial, $a_p, p = 1, \ldots, P$, is the coefficient associated with $\psi_p(\rho, \theta)$, P is the order, ρ is the normalized distance from the origin, θ is the angle, and $\varepsilon(\rho, \theta)$ represents the modeling error. Throughout the paper, we choose the polar coordinate system for convenience. It is often a requirement that the polynomials used in the modeling are orthogonal. However, after discretization, further orthogonalization using the Gram–Schmidt procedure may be required.

Using a set of such orthogonalized discrete polynomials, we can form a linear model

$$\boldsymbol{C} = \boldsymbol{\psi}\boldsymbol{a} + \boldsymbol{\varepsilon} \tag{2}$$

where $\boldsymbol{C}$ is a D-element column vector of corneal surface evaluated at discrete points (ρ_d, θ_d), $d = 1, \ldots, D$, $\boldsymbol{\psi}$ is a $(D \times P)$ matrix of discrete, orthogonalized polynomials $\psi_p(\rho_d, \theta_d)$, $\boldsymbol{a}$ is a P-element column vector of coefficients, and $\boldsymbol{\varepsilon}$ represents a D-element column vector of the measurement and modeling error. For such a model, the coefficient vector $\boldsymbol{a}$ can be estimated using the method of least-squares (LS), i.e.,

$$\hat{\boldsymbol{a}} = (\boldsymbol{\psi}^T \boldsymbol{\psi})^{-1} \boldsymbol{\psi}^T \boldsymbol{C} \tag{3}$$

where T denotes the transposition, provided that the inverse exists.

In general, corneal modeling can be put in the following framework. Given height data $C(\rho_d, \theta_d)$, $d = 1, \ldots, D$, and sampled at discrete points (ρ_d, θ_d) from $C(\rho, \theta)$ find a *complete* set of basis functions $\{\psi_p(\rho, \theta)\}$, $p = 1, 2, \ldots$, such that

$$\frac{1}{D} \sum_{d=1}^{D} \left(C(\rho_d, \theta_d) - \sum_{p=1}^{P} \hat{a}_p \psi_p(\rho_d, \theta_d) \right)^2 = \frac{1}{D} ||\boldsymbol{C} - \boldsymbol{\psi}\hat{\boldsymbol{a}}||^2 \tag{4}$$

is minimized. In other words, we are searching for a complete set of basis functions that will result in a MMSE fit to the corneal height data. In (4), $\hat{a}_p$, $p = 1, \ldots, P$ are the LS estimators of the parameters $a_p, p = 1, \ldots, P$, respectively, and $|| \cdot ||$ denotes the Euclidean norm.

III. A Repertoire of Radial Polynomials

We aim to fit the raw videokeratoscopic data with certain functions that would be a product of angular functions and radial polynomials. We would like our set of functions to be complete so that we can invoke the Weierstrass theorem on approximations. Additionally, our set of functions is to satisfy the property of invariance with respect to rotation of axis about the origin. In the following, we will consider three sets of basis functions that satisfy the above conditions: 1) the Zernike polynomials; 2) the generalized Zernike polynomials; and 3) a set of functions we choose to call Bhatia–Wolf polynomials.

TABLE I
THE RADIAL ZERNIKE POLYNOMIALS $R_n^m(\rho)$ UP TO THE DEGREE $n = 4$

Radial degree (n)	Azimuthal frequency (m) 0	1	2	3	4
0	1	—	—	—	—
1	—	2ρ	—	—	—
2	$2\rho^2 - 1$	—	ρ^2	—	—
3	—	$3\rho^3 - 2\rho$	—	ρ^3	—
4	$6\rho^4 - 6\rho^2 + 1$	—	$4\rho^4 - 3\rho^2$	—	ρ^4

A. Zernike Polynomials

A set of functions that is currently widely used in ophthalmic applications, is formed by the circle Zernike polynomials. The pth-order Zernike polynomial is defined as [10]

$$Z_p(\rho, \theta) = \begin{cases} \sqrt{2(n+1)} R_n^m(\rho) \cos(m\theta), & \text{even } p, m \neq 0 \\ \sqrt{2(n+1)} R_n^m(\rho) \sin(m\theta), & \text{odd } p, m \neq 0 \\ \sqrt{n+1} R_n^0(\rho), & m = 0 \end{cases} \tag{5}$$

where n is the radial degree, m is the azimuthal frequency, and

$$R_n^m(\rho) = \sum_{s=0}^{(n-m)/2} \frac{(-1)^s (n-s)!}{s! \left(\frac{n+m}{2} - s\right)! \left(\frac{n-m}{2} - s\right)!} \rho^{n-2s}.$$

The radial degree and the azimuthal frequency are integers which satisfy $m \leq n$ with $n - |m|$ even. Thus, only certain combinations of the coefficients n and m form valid polynomials. In Table I, we list the polynomials $R_n^m(\rho)$ up to the radial degree $n = 4$. The radial degree n and the azimuthal frequency m can be evaluated from the polynomial-ordering number p using $n = \lfloor q_1 \rfloor - 1$, and $m = q_2 + (n + (q_2 \bmod 2) \bmod 2)$ respectively, where $q_1 = 0.5(1 + \sqrt{8p - 7})$, $p = 1, \ldots, P$, $q_2 = \lfloor (n+1)(q_1 - n - 1) \rfloor$, $\lfloor \cdot \rfloor$ is the floor operator and mod denotes the modulus operator.

The Zernike polynomials have several properties that make them good candidates for fitting 2-D data:

1) they are orthogonal in x and y for the interior of the unit circle;
2) they are invariant with respect to rotation of axis about the origin, i.e.,

$$Z_p(\rho, \theta) = G_p(\phi) Z_p(\rho, \theta + \phi), \qquad p = 1, \ldots, P$$

where $G_p(\phi)$ is a continuous function with period 2π and ϕ is the angle of rotation;
3) they contain a polynomial for each permissible pair of monomials $x^i y^j$, $(i \geq 0, j \geq 0)$ (analogous property to the one of Legendre polynomials);

TABLE II
THE RADIAL GENERALIZED ZERNIKE POLYNOMIALS $S_n^m(\rho;k,l)$ UP TO THE DEGREE $n=4$, $(k_2=k/2, l_2=l/2)$

Radial degree (n)	Azimuthal frequency (m) 0	1	2	3	4
0	$\frac{\Gamma(k_2-1)}{\Gamma(l_2)}$	—	—	—	—
1	—	$\frac{\Gamma(k_2)}{\Gamma(l_2+1)}\rho$	—	—	—
2	$\frac{\Gamma(k_2+1)}{\Gamma(l_2+1)}\rho^2 - \frac{\Gamma(k_2)}{\Gamma(l_2)}$	—	$\frac{\Gamma(k_2+1)}{\Gamma(l_2+2)}\rho^2$	—	—
3	—	$\frac{\Gamma(k_2+2)}{\Gamma(l_2+2)}\rho^2 - \frac{\Gamma(k_2+1)}{\Gamma(l_2+1)}\rho$	—	$\frac{\Gamma(k_2+2)}{\Gamma(l_2+3)}\rho^3$	—
4	$\frac{\Gamma(k_2+3)}{\Gamma(l_2+2)}\rho^4 - \frac{\Gamma(k_2+2)}{\Gamma(l_2+1)}\rho^2 + \frac{\Gamma(k_2+1)}{2\Gamma(l_2)}$	—	$\frac{\Gamma(k_2+3)}{\Gamma(l_2+3)}\rho^4 - \frac{\Gamma(k_2+2)}{\Gamma(l_2+2)}\rho^2$	—	$\frac{\Gamma(k_2+3)}{\Gamma(l_2+4)}\rho^4$

TABLE III
THE RADIAL BHATIA–WOLF POLYNOMIALS $T_n^m(\rho)$ UP TO THE DEGREE $n=4$

Radial degree (n)	Azimuthal frequency (m) 0	1	2	3	4
0	1	—	—	—	—
1	$3\rho-2$	ρ	—	—	—
2	$10\rho^2-12\rho+3$	$5\rho^2-4\rho$	ρ^2	—	—
3	$35\rho^3-60\rho^2+30\rho-4$	$21\rho^3-30\rho^2+10\rho$	$7\rho^3-6\rho^2$	ρ^3	—
4	$126\rho^4-280\rho^3+210\rho^2-60\rho+5$	$84\rho^4-168\rho^3+105\rho^2-20\rho$	$36\rho^4-56\rho^3+21\rho^2$	$9\rho^4-8\rho^3$	ρ^4

4) the radial polynomials satisfy

$$\int_0^1 R_n^m(\rho)R_{n'}^m(\rho)\rho d\rho = \frac{\delta_{nn'}}{2(n+1)}$$

where $\delta_{nn'}$ is the Kronecker symbol;

5) they form a complete set of basis functions.

In some cases the Zernike polynomials $Z_p(\rho,\theta)$ are denoted as a 2-D expansion, $Z_n^{\pm m}(\rho,\theta)$ in terms of radial, n, and azimuthal, m, parameters. This is mathematically equivalent to Noll's notation and has been widely adopted by vision researchers [3]. We have chosen the Zernike polynomials proposed by Noll for convenience [12]. For the relationship between single indexing and double indexing the reader is referred to the work of VSIA Standard Taskforce [15].

B. Generalized Zernike Polynomials

There exists a number of functions that are orthogonal in a circle or a sphere [16]. However, only few sets of basis functions can satisfy properties similar to the ones of Zernike polynomials. In [17], a generalization of the radial Zernike polynomials have been considered to facilitate the evaluation of the diffraction integrals that involve products of Bessel and radial functions.

To make a correspondence with (5), we define generalized Zernike polynomials as

$$\mathcal{Z}_p(\rho,\theta;k,l) = \begin{cases} \sqrt{N(k,l,n,m)}S_n^m(\rho;k,l)\cos(m\theta), & \text{even } p, m\neq 0 \\ \sqrt{N(k,l,n,m)}S_n^m(\rho;k,l)\sin(m\theta), & \text{odd } p, m\neq 0 \\ \sqrt{\frac{N(k,l,n,m)}{2}}S_n^0(\rho;k,l), & m=0 \end{cases} \quad (6)$$

where, as in the case of the Zernike polynomials, n is the radial degree and m is the azimuthal frequency. The integers n and m can be evaluated from the polynomial-ordering number p in the same manner as described earlier for Zernike polynomials. The parameters $k>2$ and $l>0$ are additional parameters satisfying $k>l$. The radial components of the generalized Zernike polynomials are [17]

$$S_n^m(\rho;k,l) = \sum_{s=0}^{(n-m)/2} \frac{(-1)^s\Gamma\left(\frac{k}{2}+n-1-s\right)}{s!\Gamma\left(\frac{n+m+l}{2}-s\right)\left(\frac{n-m}{2}-s\right)!}\rho^{n-2s}$$

where $\Gamma(\cdot)$ is the standard gamma function. In Table II, we list the radial polynomials $S_n^m(\rho;k,l)$ up to the radial degree $n=4$.

TABLE IV
THE ZERNIKE COEFFICIENTS FOR SURFACE C (LEFT) AND THE BHATIA–WOLF COEFFICIENTS FOR SURFACE D (RIGHT)

p	Surface C Zernike coeff.	Surface D Bhatia-Wolf coeff.
1	$1.59 \cdot 10^{-1}$	$1.50 \cdot 10^{-1}$
2	$-5.59 \cdot 10^{-3}$	$-8.05 \cdot 10^{-2}$
3	$4.09 \cdot 10^{-3}$	$5.70 \cdot 10^{-3}$
4	$-7.94 \cdot 10^{-2}$	$-1.12 \cdot 10^{-4}$
5	$-3.76 \cdot 10^{-4}$	$-1.58 \cdot 10^{-2}$
6	$2.78 \cdot 10^{-3}$	$1.32 \cdot 10^{-3}$
7	$1.77 \cdot 10^{-3}$	$3.67 \cdot 10^{-3}$
8	$-4.78 \cdot 10^{-3}$	$1.04 \cdot 10^{-2}$
9	$3.99 \cdot 10^{-3}$	$5.74 \cdot 10^{-3}$
10	$-3.54 \cdot 10^{-3}$	$-1.26 \cdot 10^{-3}$
11	$4.44 \cdot 10^{-3}$	$7.28 \cdot 10^{-3}$
12	$3.99 \cdot 10^{-3}$	$9.77 \cdot 10^{-4}$
13	$6.72 \cdot 10^{-3}$	$-2.81 \cdot 10^{-3}$
14	$-5.98 \cdot 10^{-4}$	$-9.87 \cdot 10^{-3}$
15	$4.13 \cdot 10^{-4}$	$-1.27 \cdot 10^{-3}$
16		$-5.66 \cdot 10^{-5}$
17		$-2.06 \cdot 10^{-3}$
18		$-2.79 \cdot 10^{-3}$
19		$5.17 \cdot 10^{-4}$
20		$-4.66 \cdot 10^{-3}$
21		$-5.47 \cdot 10^{-3}$
22		$-5.63 \cdot 10^{-4}$
23		$8.01 \cdot 10^{-4}$
24		$6.92 \cdot 10^{-3}$
25		$-5.14 \cdot 10^{-4}$

The normalization factor used in our generalization can be calculated from the integral

$$\int_0^1 S_n^m(\rho) S_{n'}(\rho)\rho d\rho = N(k,l,n,m)\delta_{nn'}$$

and is given by

$$N(k,l,n,m) = \frac{\Gamma\left(\frac{n+m+k-2}{2}\right)\Gamma\left(\frac{n-m+k-l}{2}\right)}{(2n+k-2)\left(\frac{n-m}{2}\right)!\Gamma\left(\frac{n+m+l}{2}\right)}.$$

Substituting $k = 4$ and $l = 2$ in (6) results in the standard Zernike polynomials defined in (5).

It has been noted in [17] that such a generalization "preserves the form of the radial polynomials as originally introduced by Zernike and is adequate for most applications." However, the LS estimator of the corneal surface,

$$\hat{C}(\rho,\theta;k,l) = \sum_{p=1}^{P} \hat{a}_p(k,l)\mathcal{Z}_p(\rho,\theta;k,l)$$

results in the same fit to the data independently of the parameters k and l. This can be easily shown by expanding the matrix of the discrete generalized Zernike polynomials and grouping the common terms. Thus, the generalization of the Zernike polynomials does not provide us with an alternative modeling approach.

C. Bhatia–Wolf Polynomials

Another set of functions that is closely related to the Zernike polynomials was suggested by Bhatia and Wolf in [18]. Bhatia and Wolf sought a set of basis functions that would satisfy all of the properties of Zernike polynomials and additionally be orthogonal in x, y, *and* $\rho = \sqrt{x^2+y^2}$. This particular property is quite useful in our application, where the data are sampled radially in meridians.

We define the pth-order Bhatia–Wolf polynomial as

$$B_p(\rho,\theta) = \begin{cases} \sqrt{2(n+1)}T_n^m(\rho)\cos(m\theta), & \text{even } p, m \neq 0 \\ \sqrt{2(n+1)}T_n^m(\rho)\sin(m\theta), & \text{odd } p, m \neq 0 \\ \sqrt{n+1}T_n^0(\rho), & m = 0 \end{cases}$$

where n is the radial degree, m is the azimuthal frequency, and [18]

$$T_n^m(\rho) = \sum_{s=0}^{n-m} \frac{(-1)^s(2n+1-s)!}{s!(n-m-s)!(n+m+1-s)!}\rho^{n-s}.$$

The radial degree and the azimuthal frequency are integers which satisfy $m \leq n$. Unlike the Zernike polynomials, valid Bhatia–Wolf polynomials exist for all combinations of the coefficients n and $m \leq n$. In Table III, we list the polynomials $T_n^m(\rho)$ up to the radial degree $n = 4$. The radial degree n and the azimuthal frequency m can be evaluated from the polynomial-ordering number p using $n = \lceil\sqrt{p}\rceil - 1$ and $m = \lfloor\{p - [(n-1)^2 + 2(n-1)+1]\}/2\rfloor$, respectively, where $\lceil\cdot\rceil$ and $\lfloor\cdot\rfloor$ are the ceiling and floor operators, respectively.

The Bhatia–Wolf polynomials possess the same properties as the Zernike polynomials. Additionally, they are orthogonal in x, y, and $\rho = \sqrt{x^2+y^2}$ for the interior of the unit circle. In other words, the Bhatia–Wolf polynomial expansion will result in a series of monomials $x^i y^j \left(\sqrt{x^2+y^2}\right)^k$, $(i \geq 0, j \geq 0, k \geq 0)$. A relationship exists between the radial polynomials of Bhatia and Wolf, $T_n^m(\rho)$, and the radial polynomials of Zernike, $R_n^m(\rho)$

$$\rho T_n^m(\rho^2) = R_{2n+1}^{2m+1}(\rho).$$

Note also that Bhatia–Wolf polynomials are not a subclass of the generalized Zernike polynomials defined in (6). Since they are orthogonal in x, y, and ρ, it is expected that they would result in a better fit to the videokeratoscopic data than the Zernike polynomials of the same radial order.

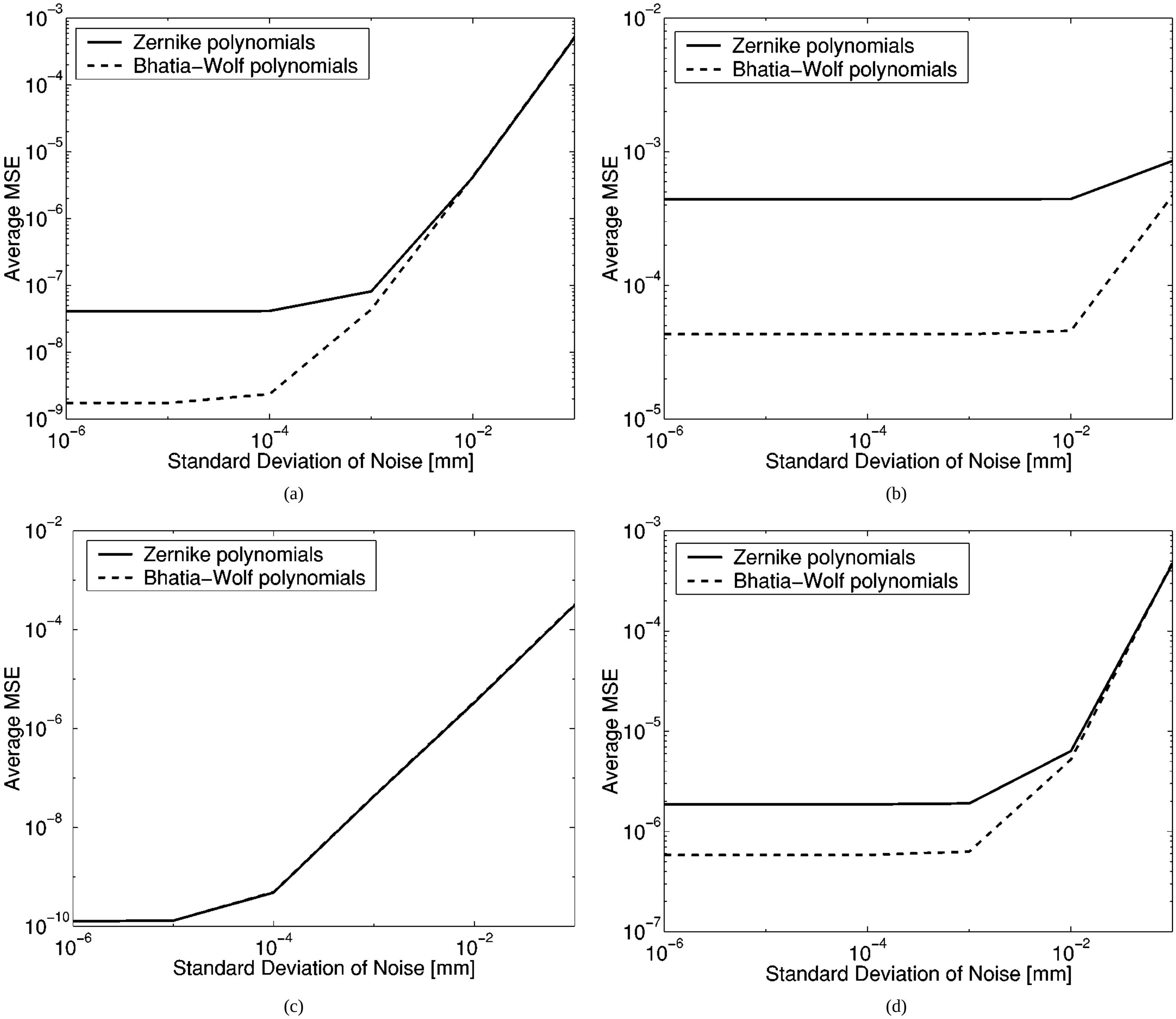

Fig. 1. Average MSE (based on 100 realizations) when fitting simulated surfaces with Zernike polynomials (solid line) and Bhatia–Wolf polynomials (dashed line). (a) Surface A—noisy sphere. (b) Surface B—noisy ellipsoid. (c) Surface C—keratoconus from Zernike terms. (d) Surface D—keratoconus from Bhatia–Wolf terms.

D. Performance Analysis

It is of interest to find how robust is the fit by Bhatia–Wolf polynomials in comparision with the Zernike polynomial fit. For this purpose we have chosen the following four simulated surfaces.

1) Surface A: a sphere with radius $r = 7.8$ mm;
2) Surface B: an ellipsoid with $a = 3r$ and $b = 2r$;
3) Surface C: a keratoconic corneal surface modeled by a series of the first 15 Zernike polynomials (up to the fourth radial order, see Table IV);
4) Surface D: a keratoconic corneal surface modeled by a series of the first 25 Bhatia–Wolf polynomials (up to the fourth radial order, see Table IV).

We proceed with our analysis as follows. First, we generate each surface at discrete points (ρ_d, θ_d), $d = 1, \ldots, D$. We choose 256 semimeridians, 26 rings, and $\rho_{\max} = 4$ mm. Then we collect the discrete elevation data into a vector $\boldsymbol{C}_0$. To each of the simulated surfaces, independent and identically distributed zero-mean Gaussian noise is added, $\boldsymbol{C} = \boldsymbol{C}_0 + \boldsymbol{N}$. The standard deviation of noise ranges from 1 nm to 100 μm. The level of noise found in current videokeratoscopes is usually a couple of microns [14]. Then, we find LS estimators of the surfaces using

$$\hat{\boldsymbol{C}}_{\mathrm{Z}} = \boldsymbol{Z}\hat{\boldsymbol{a}}$$

and

$$\hat{\boldsymbol{C}}_{\mathrm{BW}} = \boldsymbol{B}\hat{\boldsymbol{b}}$$

where

$$\hat{\boldsymbol{a}} = \left(\boldsymbol{Z}^T\boldsymbol{Z}\right)^{-1}\boldsymbol{Z}^T\boldsymbol{C} \text{ and } \hat{\boldsymbol{b}} = \left(\boldsymbol{B}^T\boldsymbol{B}\right)^{-1}\boldsymbol{B}^T\boldsymbol{C}$$

with $\boldsymbol{Z}$ being a $(D \times 15)$ matrix of discrete Zernike polynomials, and $\boldsymbol{B}$ being a $(D \times 25)$ matrix of discrete Bhatia–Wolf polynomials. Next, we calculate the mean square errors (MSEs)

$$\mathsf{MSE}_{\mathrm{Z}} = \frac{1}{D}||\boldsymbol{C}_0 - \hat{\boldsymbol{C}}_{\mathrm{Z}}||^2 \text{ and } \mathsf{MSE}_{\mathrm{BW}} = \frac{1}{D}||\boldsymbol{C}_0 - \hat{\boldsymbol{C}}_{\mathrm{BW}}||^2.$$

We repeat this procedure for 100 independent realizations of the noise process and calculate the average of the MSE's. In Fig. 1(a) and (b), we show the average $\mathsf{MSE}_{\mathrm{Z}}$ (solid line) and $\mathsf{MSE}_{\mathrm{BW}}$ (dashed line) for Surface A and Surface B, respectively. It is noted that for the range of noise encountered in current videokeratoscopes, the Bhatia–Wolf polynomial fit results in a much better model to a sphere or an ellipsoid than the Zernike polynomial fit. It is also interesting that for a very high level of noise both representations provide similar fit.

The two other simulated surfaces where used to establish the robustness of the corneal fit. Fig. 1(c) and (d) shows the average $\mathsf{MSE}_{\mathrm{Z}}$ and $\mathsf{MSE}_{\mathrm{BW}}$ for Surface C and Surface D, respectively. It is of interest to note that in the mean-square error sense, the Bhatia–Wolf polynomials provide the same fit to the surfaces generated by the Zernike polynomials as the Zernike polynomials themselves [see Fig. 1(c)]. However, the same cannot be said about the Zernike polynomials when used for fitting surfaces generated by the Bhatia–Wolf polynomials [see Fig. 1(d)]. Thus, the Bhatia–Wolf polynomials are more robust than the Zernike polynomials of equivalent radial order.

Note also, that the flat components of the average MSE in Fig. 1 are related to systematic errors related to the fit, while the increases in the MSE at a certain noise level are related to statistical errors.

IV. Experimental Results

In this section, we provide examples of fitting Zernike polynomials and Bhatia–Wolf polynomials to corneal elevation data. We did not include the analysis of the generalized Zernike polynomials since, for a given order, they result in an identical LS estimate of the corneal surface as in the case of the Zernike polynomials.

The elevation data was measured by the Optikon Keratron videokeratoscope. The size of the Keratron data is $D = 6656$. The data are sampled in 256 semimeridians (approximately every 1.4°) and 26 rings, covering up to 9-mm diameter of a corneal surface.

From the results derived in [12], [13] we choose to model each corneal elevation with a radial polynomial of order $n = 4$. This corresponds to modeling a corneal surface with the first 15 Zernike polynomials or the first 25 Bhatia–Wolf polynomials.

Consider first a set of typical videokeratoscopic data from a healthy normal cornea (Subject A). We select the 8-mm diameter central portion of the corneal data for the analysis because the peripherial data (the last two rings) are usually not suitable for the analysis. In Fig. 2, we show typical set of raw elevation data from the Keratron videokeratoscope for 8-mm corneal diameter. Some of the data in the most outer rings may be missing due to occlusion by the eye-lids or lashes.

Local changes in corneal elevation are too small relative to its principal curvature, similar to the geographical features of the Earth when viewed from space. Thus, to visualize such changes, the residual elevation data are often used. These are calculated by subtracting the best fit sphere (in the LS sense) from the elevation data. Fig. 3 shows the residual elevation data for Subject A.

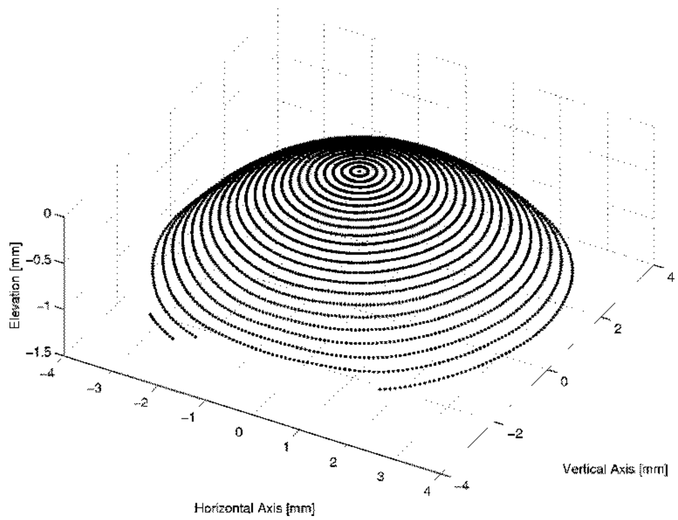

Fig. 2. Raw elevation data from the Keratron videokeratoscope for 8-mm corneal diameter.

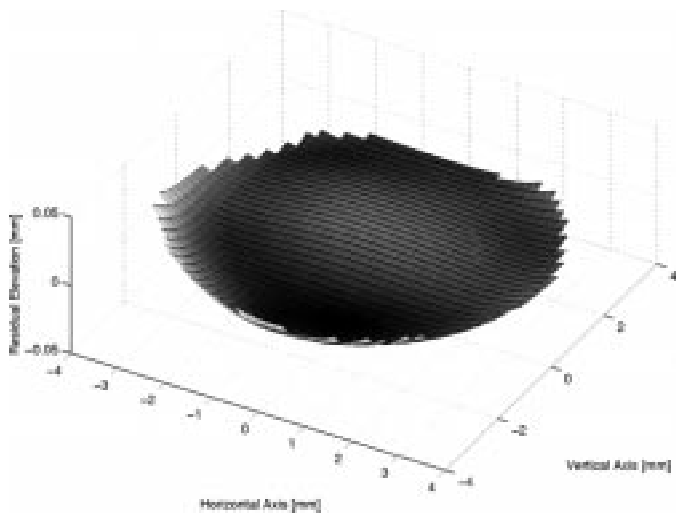

Fig. 3. Residual elevation data (difference between the elevation and the best fit sphere) for Subject A with normal cornea.

We repeat the procedure from the previous section omitting the addition of the noise. Second, we define the residual modeling errors as

$$\hat{\varepsilon}_{\mathrm{Z}} = \boldsymbol{C} - \hat{\boldsymbol{C}}_{\mathrm{Z}} \text{ and } \hat{\varepsilon}_{\mathrm{BW}} = \boldsymbol{C} - \hat{\boldsymbol{C}}_{\mathrm{BW}}.$$

In Fig. 4, we show the residual modeling errors for the Zernike polynomial fit (top) and Bhatia–Wolf polynomial fit (bottom). A decrease in the MSE from $\mathsf{MSE}_{\mathrm{Z}} = 4.23 \times 10^{-7}$ to $\mathsf{MSE}_{\mathrm{BW}} = 2.53 \times 10^{-7}$ was found.

We have continued the analysis with three other subjects: Subject B with significant amount of astigmatism, Subject C with topographic asymmetry (early keratoconus), and Subject

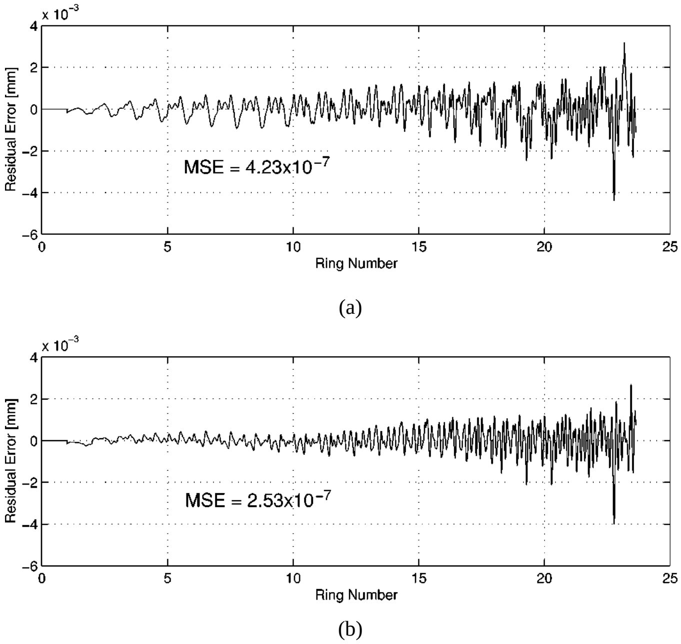

Fig. 4. Residual modeling error for cornea of Subject A fitted by (a) a series of Zernikes polynomials and (b) a series of Bhatia–Wolf polynomials.

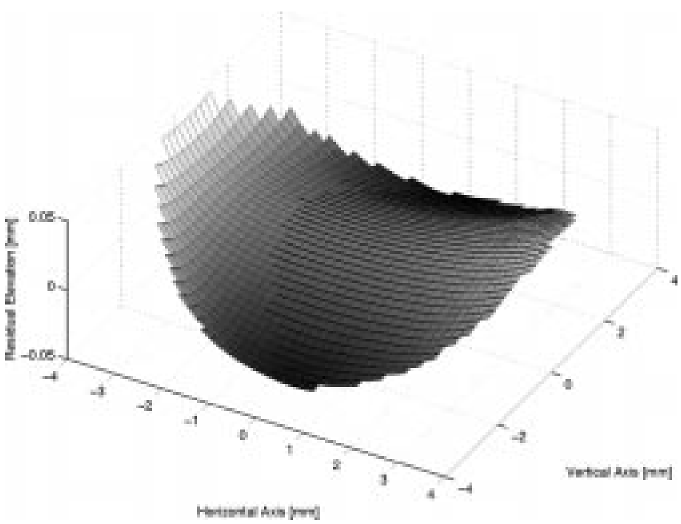

Fig. 5. Residual elevation data (difference between the elevation and the best fit sphere) for Subject B with corneal astigmatism.

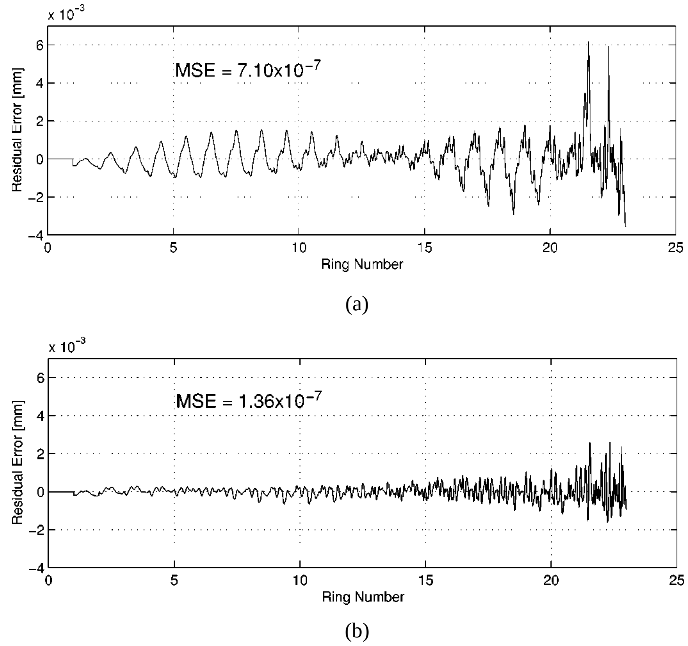

Fig. 6. Residual modeling error for cornea of Subject B fitted by (a) a series of Zernikes polynomials and (b) a series of Bhatia–Wolf polynomials.

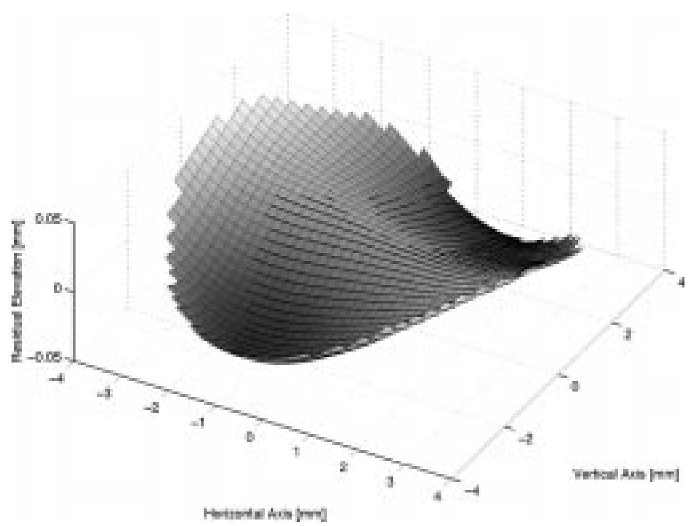

Fig. 7. Residual elevation data (difference between the elevation and the best fit sphere) for Subject C with topographic asymmetry (early keratoconus).

D with a significantly decentered corneal apex (severe keratoconus). Figs. 5 and 6 show the residual elevation and residual modeling error for Subject B. Similarly, Figs. 7–10 show the residual elevation and residual modeling error for Subject C and Subject D, respectively.

As noted for the normal cornea, a decrease in the MSE is evident when modeling corneal surfaces with Bhatia–Wolf polynomials. Also, for corneal surfaces with significant deformities, the decrease in the MSE is more pronounced than in the case of normal corneas. For example, for Subject D, the decrease in the MSE is tenfold.

Worth noting is that in most cases the residual modeling error for the Bhatia–Wolf polynomial fit is in close agreement with the results obtained when testing videokeratoscopes with artificial surfaces [14]. In comparison, the Zernike polynomial fit with the same radial order results in a residual modeling error that exceeds that of the artificial surfaces.

We have perfomed a comparison between the Zernike polynomial fit and the Bhatia–Wolf polynomial fit for 70 subjects including 60 normals (some with astigmatism) and ten subjects with keratoconus. For each cornea, we have determined the $\mathrm{MSE}_{\mathrm{Z}}$ and $\mathrm{MSE}_{\mathrm{BW}}$. Fig. 11 shows the MSE for the Bhatia–Wolf polynomials versus the MSE for the Zernike polynomial fit. It is clear that the $\mathrm{MSE}_{\mathrm{BW}}$ is consistently lower than the $\mathrm{MSE}_{\mathrm{Z}}$ for all considered subjects. Also, it is of interest that for a small corneal diameter, the Bhatia–Wolf polynomial fit is much better than the Zernike polynomial fit. This advantage is important when deriving aberrations for corneal areas related to the pupil.

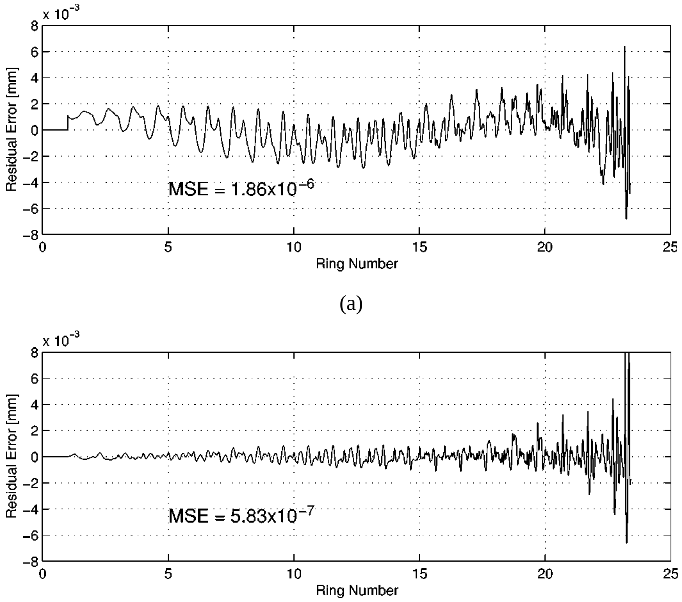

(a)

(b)

Fig. 8. Residual modeling error for cornea of Subject C fitted by (a) a series of Zernikes polynomials and (b) a series of Bhatia–Wolf polynomial.

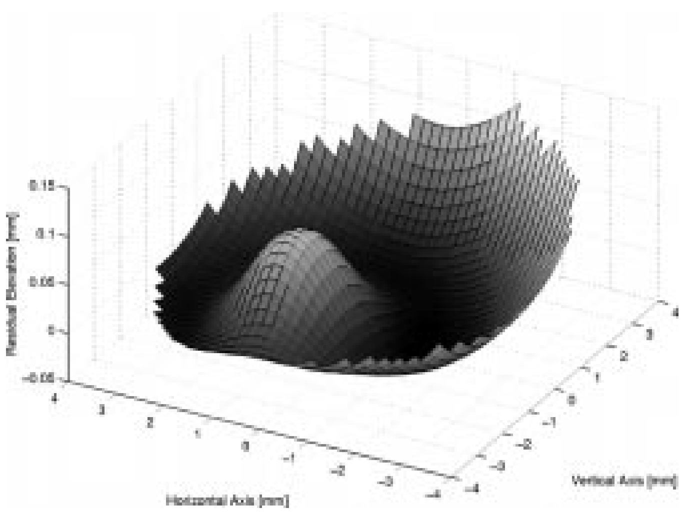

Fig. 9. Residual elevation data (difference between the elevation and the best fit sphere) for Subject D with a decentered corneal apex (severe keratoconus).

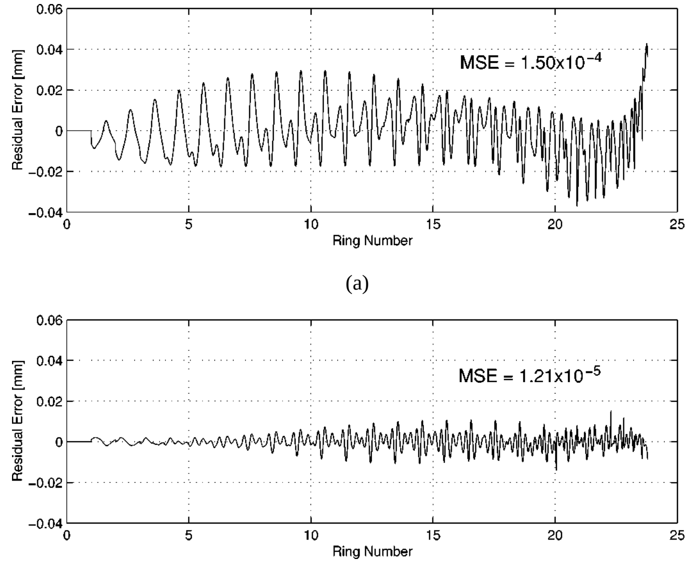

(a)

(b)

Fig. 10. Residual modeling error for cornea of Subject D fitted by (a) a series of Zernikes polynomials and (b) a series of Bhatia–Wolf polynomials.

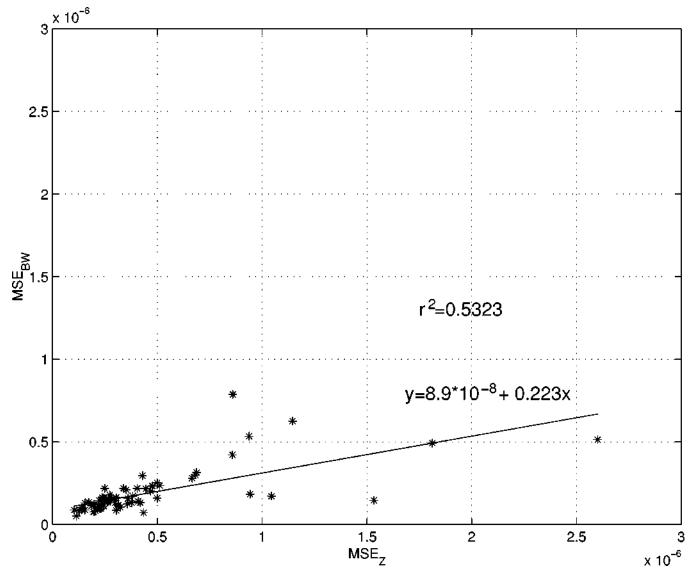

Fig. 11. MSE for the Bhatia–Wolf polynomial fit versus the MSE for the Zernike polynomial fit for 70 different corneas.

V. Conclusion

We have introduced a new model, referred to as the Bhatia–Wolf polynomial expansion, for fitting the videokeratoscopic height data of the anterior corneal surface. Given certain order of the radial polynomial expansion, the Bhatia–Wolf polynomials significantly outperform the widely used set of Zernike polynomials in terms of the MSE fit. This was shown for simulated data as well as data from real corneas of subjects with different corneal topographies. Also, we showed that Bhatia–Wolf polynomials provide a robust fit to the corneal data.

The Bhatia–Wolf polynomial fit of a certain radial order n is numerically less efficient than the equivalent Zernike polynomial fit. However, comparison of the fitting performance using the same number of polynomial terms in both polynomial expansions could not be justified because it will result in different radial orders for each of the expansions.

The proposed methodology can be also used for fitting wavefront aberrations as measured by a wavefront sensor. Although some of the lower order terms of the Bhatia–Wolf polynomial expansion may not be directly recognized as a commonly known type of aberration, their use in fitting could provide a significant improvement in wavefront estimation. This is particularly important in areas such as customized refractive surgery, where the information from the Zernike polynomial fit may be used for corneal ablation. The analysis of this problem is beyond the scope of this paper and will be reported elsewhere.

REFERENCES

[1] R. A. Applegate and H. C. Howland, "Noninvasive measurement of corneal topography," *IEEE Eng. Med. Biol. Mag.*, vol. 14, pp. 30–42, Jan./Feb. 1995.

[2] R. B. Mandell, "A guide to videokeratography," *Int. Contact Lens Clin.*, vol. 23, no. 6, pp. 205–228, 1996.

[3] J. Schweigerling and J. E. Greivenkamp, "Using corneal height maps and polynomial decomposition to determine corneal aberrations," *Opt. Vis. Sci.*, vol. 74, no. 11, pp. 906–916, 1997.

[4] A. Guirao and P. Artal, "Corneal wave aberration from videokeratography: Accuracy and limitations of the procedure," *J. Opt. Soc. Am. A*, vol. 17, no. 6, pp. 955–965, 2000.

[5] J. Schweigerling and J. E. Greivenkamp, "Keratoconus detection based on videokeratoscopic height data," *Opt. Vis. Sci.*, vol. 73, no. 12, pp. 721–728, 1996.

[6] A. Langenbucher, B. Seitz, M. M. Kus, and G. O. H. Naumann, "Zernike representation of corneal topography height data after nonmechanical penetrating keratoplasty," *Investigat. Ophthal. Vis. Sci.*, vol. 40, no. 3, pp. 582–591, 1999.

[7] W. Lotmar, "Theoretical eye model with aspherics," *J. Opt. Soc. Amer.*, vol. 61, pp. 1522–1529, 1971.

[8] J. Schwiegerling, J. E. Greivenkamp, and J. M. Miller, "Representation of videokeratoscopic height data with Zernike polynomials," *J. Opt. Soc. Amer. A*, vol. 12, no. 10, pp. 2105–2113, 1995.

[9] M. Born and E. Wolf, *Principles of Optics*, 7th ed. Cambridge, U.K.: Cambridge Univ. Press, 1999.

[10] R. J. Noll, "Zernike polynomials and atmospheric turbulence," *J. Opt. Soc. Amer.*, vol. 66, no. 3, pp. 207–211, 1976.

[11] S. S. Dalal, S. A. Klein, B. A. Barsky, and J. C. Corzine, "Limitations to the Zernike representation of cornea and wavefront for post-refractive surgery eyes, (ARVO abstract)," *Investigat. Ophthal. Vis. Sci.*, vol. 42, no. 4, p. S603, 2001.

[12] D. R. Iskander, M. J. Collins, and B. Davis, "Optimal modeling of corneal surfaces with Zernike polynomials," *IEEE Trans. Biomed. Eng.*, vol. 48, pp. 85–97, Jan. 2001.

[13] D. R. Iskander, M. J. Collins, B. Davis, and R. Franklin, "Corneal surface characterization: How many Zernike terms should be used? (ARVO abstract)," *Investigat. Ophthal. Vis. Sci.*, vol. 42, no. 4, p. S896, 2001.

[14] W. Tang, M. J. Collins, L. Carney, and B. Davis, "The accuracy and precision performance of four videokeratoscopes in measuring test surfaces," *Opt. Vis. Sci.*, vol. 77, no. 9, pp. 483–491, 2000.

[15] L. N. Thibos, R. A. Applegate, J. T. Schwiegerling, and R. Webb. Standards for reporting the optical aberrations of eyes. presented at Vision Science and its Applications Conf.. [Online]. Available: http://www.osa.org/Homes/vision/resources/intro.htm

[16] A. Erdélyi *et al.*, *Higher Transcendental Functions*. New York: McGraw Hill, 1953, vol. II, ch. XII.

[17] D. R. Myrick, "A generalization of the radial polynomials of F. Zernike," *J. SIAM Appl. Math.*, vol. 14, no. 3, pp. 476–489, 1966.

[18] A. B. Bhatia and E. Wolf, "On the circle polynomials of Zernike and related orthogonal sets," in *Proc. Cambridge Philos. Soc.*, vol. 50, 1954, pp. 40–53.

D. Robert Iskander (M'98) received the Magister Inżynier degree in electronic engineering from the Technical University of Lodz, Poland, in 1991, and the Ph.D. degree in signal processing from Queensland University of Technology (QUT), Queensland, Australia, in 1997.

From 1996 to 2000, he was a Research Fellow at the Signal Processing Research Centre, the Cooperative Research Centre for Satellite Systems, and the Centre for Eye Research, QUT. In 2001, he joined the School of Engineering, Griffith University, Brisbane, as a Senior Lecturer. He is also a Visting Research Fellow at the Centre for Eye Research, QUT, and an Associate Member of the Communications and Signal Processing Group at Curtin University of Technology, Perth, Australia. His current research interests include statistical signal processing, visual optics, and optometry.

Dr Iskander is a member of the Association for Research in Vision and Ophthalmology.

Mark R. Morelande received the B.Eng. in aerospace avionics from Queensland University of Technology, Brisbane, Australia, in 1997 and the Ph.D. in electrical engineering from Curtin University of Technology, Perth, Australia in 2001.

Since March 2001 he has been employed as a Research Fellow at the Centre for Eye Research, Queensland University of Technology where he develops and applies signal processing techniques to various problems in visual optics.

Michael J. Collins received the Dip.App.Sc. (Optom), M.App.Sc., and Ph.D. degrees from Queensland University of Technology, Brisbane, Australia, in 1977, 1988, and 1996, respectively.

He is an Associate Professor in the School of Optometry at the Queensland University of Technology. His research laboratory, the Contact Lens and Visual Optics Laboratory, specialises in the visual and optical characteristics of the cornea and contact lenses.

Dr. Collins is a member of the Optometrists Association of Australia, Fellow of the American Academy of Optometry, a Fellow of the Contact Lens Society of Australia and a member of the International Society for Contact Lens Research.

Brett Davis received the Bachelor of Applied Science (Physics) from Queensland University of Technology (QUT), Brisbane, Australia, in 1990.

He is a Senior Research Assistant in the Centre for Eye Research at QUT. He has been involved in various research projects within the Contact Lens and Visual Optics Laboratory, Centre for Eye Research, at QUT. His interests include visual optics and optical design.